Supplementary Material for
A new methodology for a detailed investigation of quantized friction in ionic liquids

Romain Lhermerout[1] and Susan Perkin[1]
Department of Chemistry, Physical and Theoretical Chemistry Laboratory, University of Oxford, Oxford OX1 3QZ, UK

I. DISCUSSION OF LIQUID-LIKE AND SOLID-LIKE FRICTION RESPONSE

In the present work the friction traces indicate liquid-like response of the film under shear, which contrasts with previous SFB experiments performed with the same ionic liquid in our group[1]. In this previous work, a solid-like friction behavior was observed instead, i.e. a lateral force showing a stiction spike, followed by a stick-slip process at small velocities ($v_\mathrm{L} \in [200; 500]$ nm/s) or a smooth-sliding plateau at large velocities ($v_\mathrm{L} \in [500; 1000]$ nm/s). In the following, we enumerate and discuss several reasons that could explain this discrepancy.

- **Mechanical parameters.** For various physico-chemical systems (self-assembled monolayers in dry contact, mica surfaces separated by apolar or ionic liquids etc.), it has been found that the occurrence of stick-slip or smooth sliding after the stiction spike depends on the lateral velocity, the load and the number of layers composing the film[1–8]. Here, we have no stiction spike and smooth sliding in the whole ranges of lateral velocities $v_\mathrm{L} \in [30; 3000]$ nm/s, loads $F_\mathrm{N} \in [-0.20; 5.00]$ mN (ranges including the values used in[1]), and for all the distinguishable layers.

- **Vibrations.** It has been shown that stiction and stick-slip can be reduced or even suppressed by external mechanical vibrations[9–14]. The SFB used here is similar to the one in[1], with the same piezoelectric tube to produce the motions, and equivalent passive and active elements to damp external vibrations. The noise on the lateral force signal is similar, with a spectrum up to 500 Hz dominated by the resonance of the mass-spring system at $\sim$ 20 Hz (see the tiny oscillation in inset of Figure 3). Furthermore, the friction behavior is not affected whether a simultaneous normal motion is imposed or not with the piezoelectric tube.

- **Humidity.** A transition from solid-like to liquid-like friction behavior by addition of water traces has been observed for apolar liquids and ionic liquids[15,16]. Here, we have performed the measurements in dry or wet conditions (following procedures given in subsection 2.2), and systematically observed a liquid-like friction behavior.

- **Mica orientation.** For various confined fluids (gases, apolar liquids, aqueous electrolytes, liquid crystals etc.), the relative orientation of the two crystalline mica surfaces has been proved to affect the amplitude of adhesion and friction forces, or even to induce a transition from solid-like behavior to liquid-like behavior[15,17–20]. Such scenario is likely to also happen for ionic liquids, and could explain the opposite observations made in the present study and in[1].

In light of this discussion, the effect of mica orientation appears to be the best candidate to explain our observation of a liquid-like -and not solid-like- friction behavior.

II. INFLUENCE OF LATERAL ORGANISATION

Here we comment on some observations made during this study of the quantitative reproducibility of ours results. For clarity, the data shown in this paper are only a part of all the data collected. In fact, the measurements have been performed in several experiments (different pairs of mica surfaces and liquid) and at different contact spots on the mica surfaces. Essentially, we found a good reproducibility for normal force measurements, and a greater variability for lateral force measurements. To illustrate this point, Supplementary Figure 7 shows the measurements done with wet $[C_4C_1Pyrr][NTf_2]$, during the same experiment described in subsection 3.4 (in main text), but at a different contact spot while keeping the same relative orientation of the mica surfaces within a few degrees. Qualitatively, the phenomenology is similar, as we observe a structural force profile, a liquid-like friction behavior, a quantized friction-load relationship, and a friction coefficient that significantly increases with the shearing velocity in layer $i = 2$. Quantitatively, the structural force profile is similar, with in particular the squeeze-out transition from layer $i = 2$ to layer $i = 1$ that happens at a load of same order of magnitude $F_\mathrm{N} = 4.72$ mN (corresponding to a pressure $\sim$

$F_N/(\pi a^2) \sim 6$ MPa, given a contact radius $a = 16.38$ μm). However, the friction coefficients are about one order of magnitude smaller, $\mu_1 = 0.065 \pm 0.001$, $\mu_2 = 0.0048 \pm 0.0001$ and $\mu_3 = 0.0005 \pm 0.0004$! Also intriguing, a really good fit of the friction-load relationship with equation 4 (in main text) is obtained when supposing a purely contact area-controlled, with $\{\sigma_{c,1} = 377.7 \pm 0.6$ kPa, $F_1^{min} = -0.15$ mN$\}$. Adding the other term proportional to the load does not improve significantly the fit, and is reflected on the uncertainty on the friction coefficient: $\{\mu_1 = 0.0013 \pm 0.0010$, $\sigma_{c,1} = 371 \pm 5$ kPa, $F_1^{min} = -0.15$ mN$\}$. The friction measurements could be reproduced many times for a given contact spot, but changed immediately after changing the contact spot. All the other control parameters were kept constant: nature of the system (surfaces and liquid preparation, geometry), mechanical parameters (load, velocities), level of vibrations, humidity, relative orientation of the mica surfaces, etc. A possible interpretation is that the structural force is only sensitive to the film structure in the normal direction, whereas the friction force is determined by the film structure in the normal and lateral directions. In the vicinity of a single mica surface, the ions of the ionic liquid are known to be ordered in normal and lateral directions, forming possibly large domains of uniform orientation. When changing the contact spot while keeping the same relative orientation of the mica surfaces and the same sliding direction, different domains or sets of domain may be probed, with a small effect on structural force but a dramatic influence on friction.

Such variability on the lateral force measurements has to be considered when comparing quantitatively the friction performances of different systems. It is for example the case when investigating the effect of humidity on the lubricity of ionic liquids. In a previous SFB experiment using $[C_{10}C_1Im][NTf_2]$, 1-decyl-1-methylpyrrolidinium *bis*[(trifluoromethane)sulfonyl]imide[21], and a previous AFM experiments using $[C_2C_1Im][EtSO_4]$, 1-ethyl-3-methylimidazolium ethylsulfate, or $[C_2C_1Im][FAP]$, 1-ethyl-3-methylimidazolium *tris*(pentafluoroethyl)trifluorophosphate, or $[C_6C_1Im][FAP]$, 1-hexyl-3-methylimidazolium *tris*(pentafluoroethyl)trifluorophosphate[22], the friction coefficients of the different layers have been found to increase by addition of water. A similar trend has been found with molecular dynamics simulations, interpreted by a shift of the slippage plane in the gap[23]. In our study, we find an increase of the friction coefficients with humidity when comparing the results in dry conditions (Figure 4 in main text) with the results in wet conditions on a first contact spot (Figure 5 in main text), or a decrease of the friction coefficients with humidity when comparing the results in dry conditions (Figure 4 in main text) with the results in wet conditions on a second contact spot (Supplementary Figure 7). In fact, the friction coefficients vary more by changing the contact spot than by adding water traces, making impossible to conclude. A quantitative investigation of the effect of water on the lubricity of ionic liquids would require to measure friction at different humidity levels on the same contact spot, and then to reproduce this procedure on several contact spots. Nevertheless, an equivalent attention would have to be dedicated to understand the effect of changing the contact spot, which can be of larger magnitude.

III. SUPPLEMENTARY FIGURES

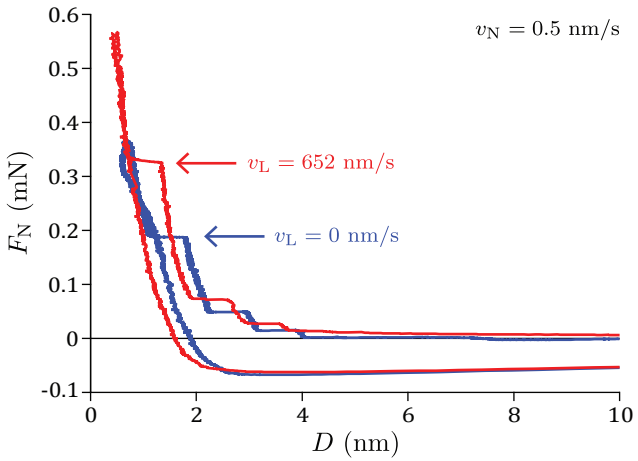

FIG. 1. Measurements for dry $[C_4C_1Pyrr][NTf_2]$ ($R = 0.92$ cm). Normal force profiles when moving the top surface with the piezoelectric tube at a normal velocity $v_N = 0.5$ nm/s (full approach, then retraction from layer $i = 1$) and a lateral velocity $v_L = 652$ nm/s (in red) or $v_L = 0$ nm/s (in blue). The two structural force profiles are reasonably similar, given the usual reproducibility on such delicate measurements, ruling out any substantial modification of the liquid structure by the shearing motion.

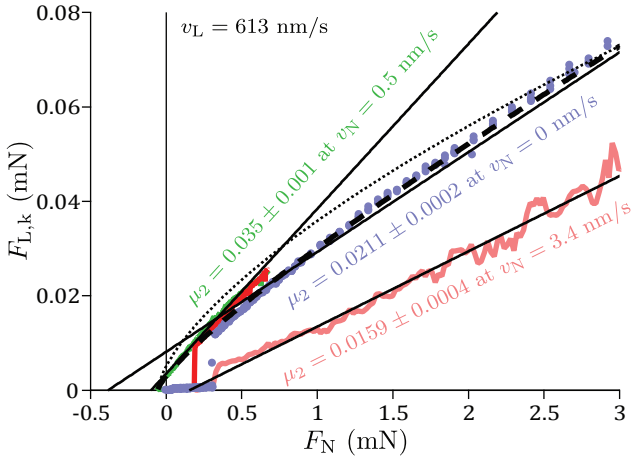

FIG. 2. Measurements for wet $[C_4C_1Pyrr][NTf_2]$ ($R = 1.45$ cm). Kinetic friction $F_{L,k}$ as a function of load F_N, when shearing the liquid at $v_L = 613$ nm/s (i) while approaching then retracting the surfaces with the piezoelectric tube at $v_N = 0.5$ nm/s (in red and green), (ii) or while approaching the surfaces by discrete steps with the stepper motor (in faded blue), (iii) or while approaching the surfaces continuously with the stepper motors at $v_N = 3.4$ nm/s (in faded red). Straight lines are fits in layer $i = 2$ with the left-hand term of equation 4 (in main text), respectively giving $\{\mu_2 = 0.035 \pm 0.001,\ F_2^{\min} = -0.101 \pm 0.004$ mN$\}$, $\{\mu_2 = 0.0211 \pm 0.002,\ F_2^{\min} = -0.39 \pm 0.02$ mN$\}$ and $\{\mu_2 = 0.0159 \pm 0.004,\ F_2^{\min} = -0.15 \pm 0.05$ mN$\}$. The dotted line is a fit in layer $i = 2$ for the approach by discrete steps with the right-hand term of equation 4 (in main text), with $\{\sigma_{c,2} = 121 \pm 2$ kPa, $F_2^{\min} = -0.06$ mN$\}$. The dashed line is a fit in layer $i = 2$ for the approach by discrete steps with the whole equation 4 (in main text), with $\{\mu_2 = 0.0129 \pm 0.003,\ \sigma_{c,2} = 56 \pm 2$ kPa, $F_2^{\min} = -0.06$ mN$\}$. The continuous approach with the piezoelectric tube (i) is reasonably similar to the discrete approach with the stepper motor (ii), given the usual reproducibility on such delicate measurements, ruling out any substantial modification of the friction force by mechanical vibrations (potentially induced by the simultaneous normal motion with the piezoelectric tube). The continuous approach with the stepper motor (iii) also exhibit quantized friction with a similar friction coefficient, but the signal is much noisier and the amplitude of the friction force is significantly smaller. The simultaneous normal motion with the stepper motor induces mechanical vibrations, which in turn reduce the friction force. Using the stepper motor for the continuous approach therefore provides qualitative -and not quantitative- measurements.

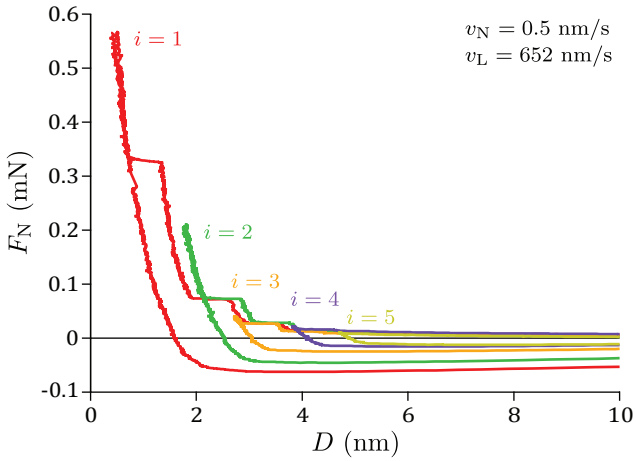

FIG. 3. Measurements for dry $[C_4C_1Pyrr][NTf_2]$ ($R = 0.92$ cm). Normal force profile when moving the top surface with the piezoelectric tube at a normal velocity $v_N = 0.5$ nm/s and a lateral velocity $v_L = 652$ nm/s, showing structuring with 5 distinguishable layers labeled by i. The different colors stand for approach up to a given layer and retraction from this layer: $i = 1$ in red, $i = 2$ in green, $i = 3$ in orange, $i = 4$ in purple, and $i = 5$ in yellow. From run to run, the whole force profile randomly shifts by a fraction of nanometer, as a result of imperfections of the set-up (like tiny rotations of the solids).

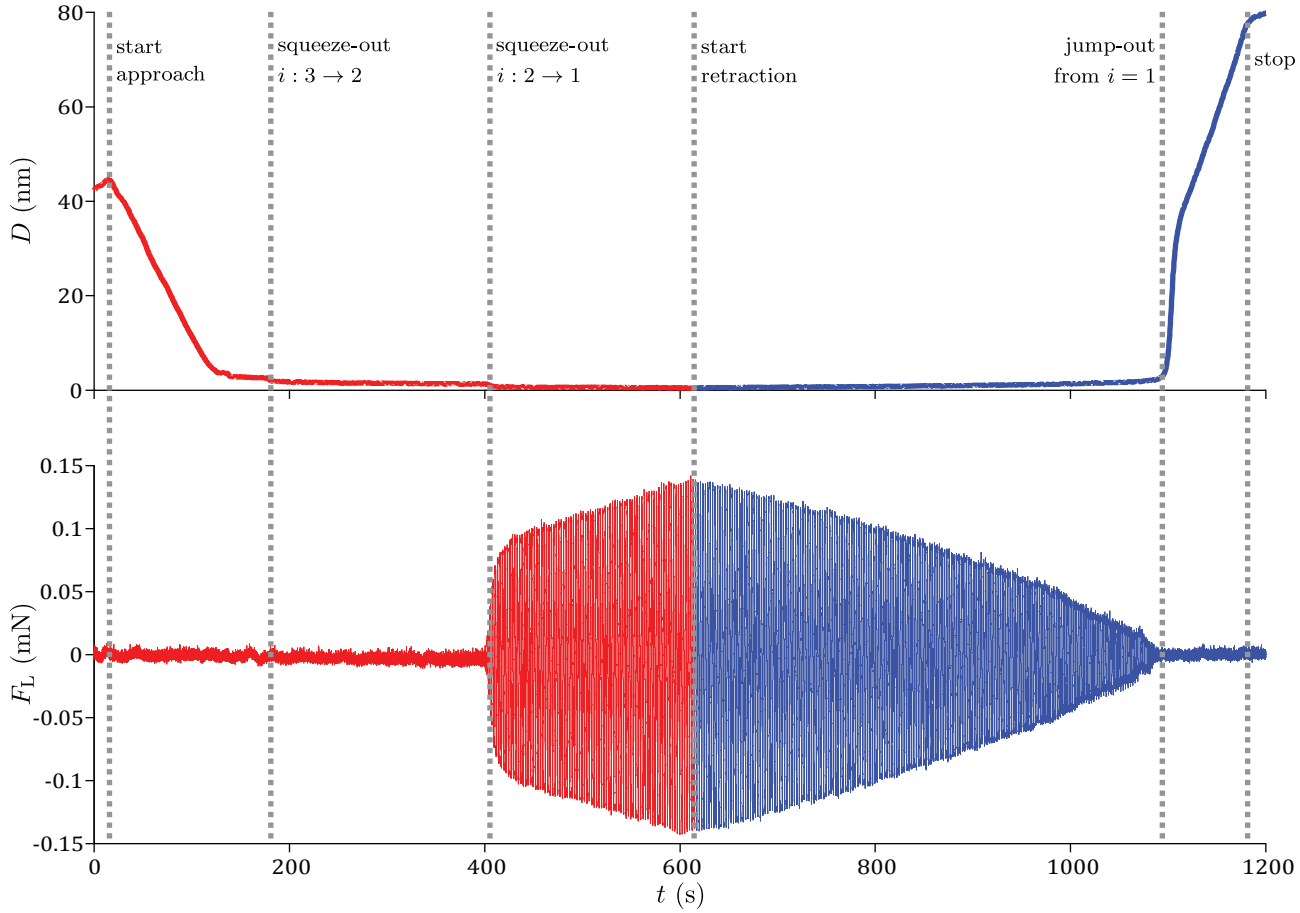

FIG. 4. Measurements for dry $[C_4C_1Pyrr][NTf_2]$ ($R = 0.92$ cm). Temporal evolutions of the apical distance D and lateral force F_L, when moving the top surface with the piezoelectric tube at a normal velocity $v_N = 0.5$ nm/s and a lateral velocity $v_L = 652$ nm/s. At time $t \sim 0$ s, approach is started and friction is below the sensitivity limit. The liquid film decreases roughly linearly at large distances, then layer by layer at short distances ($D \lesssim 5$ nm). At $t \sim 200$ s, the layer $i = 2$ is reached, friction becomes measurable and increases with the load (not visible at this scale, but discernible in inset of Figure 4(a) in main text). At $t \sim 400$ s, the layer $i = 1$ is reached, friction is much larger and clearly increases with the load. At time $t \sim 600$ s, retraction is started, and friction decreases with the load. At $t \sim 1100$ s, the adhesive minimum is reached, friction simultaneously becomes non measurable again, and the surfaces jump-out. The liquid film then increases roughly linearly at large distances, until the motion is stopped at $t \sim 1200$ s.

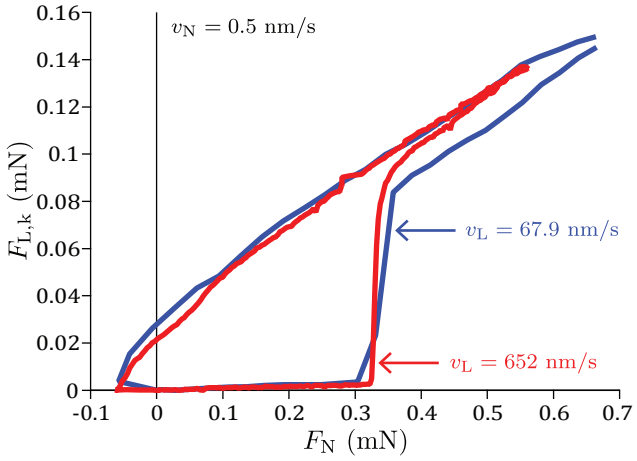

FIG. 5. Measurements for dry $[C_4C_1Pyrr][NTf_2]$ ($R = 0.92$ cm). Kinetic friction $F_{L,k}$ as a function of load F_N, when moving the top surface with the piezoelectric tube at a normal velocity $v_N = 0.5$ nm/s (full approach, then retraction from layer $i = 1$) and a lateral velocity $v_L = 652$ nm/s (in red) or $v_L = 67.9$ nm/s (in blue). The two friction-load relationships are reasonably similar, given the usual reproducibility on such delicate measurements, showing that for this system the friction force has no measurable dependence on the lateral velocity, over the range of lateral velocities explored.

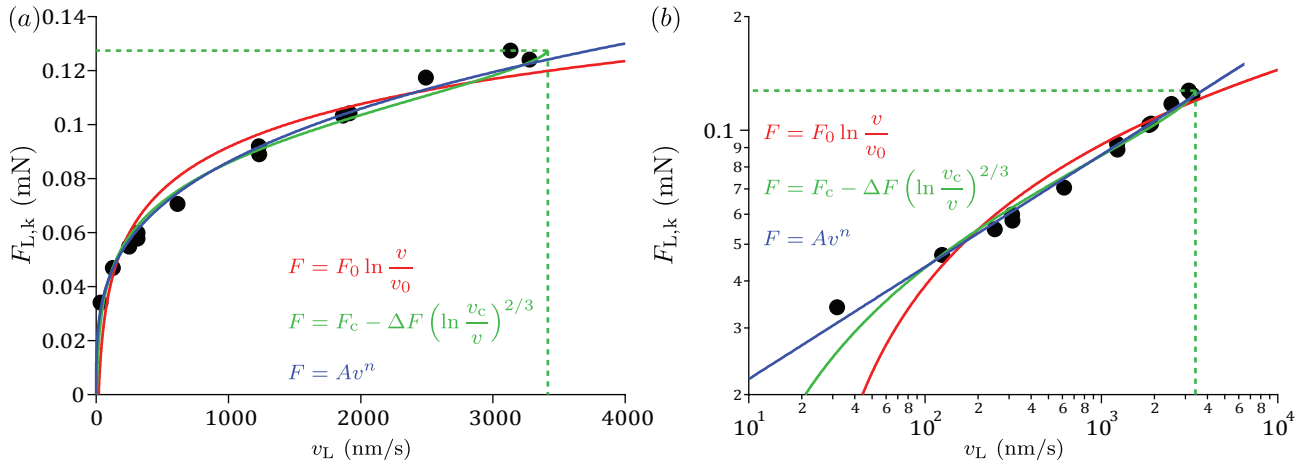

FIG. 6. Measurements for wet $[C_4C_1Pyrr][NTf_2]$ ($R = 1.45$ cm), at fixed load $F_N = 2.79$ mN, distance $D = -1.05$ nm (where $D = D_{liquid} - 2\delta e_{mica} < 0$) and contact radius $a = 12.86$ μm in layer $i = 2$. Kinetic friction $F_{L,k}$ as a function of lateral velocity v_L, in (a) lin-lin and (b) log-log representations. The red curve is a fit with equation 5 (in main text) giving $\{F_0 = (23\pm4)\cdot10^{-3}$ mN, $v_0 = 18\pm10$ nm/s$\}$. The green curve is a fit with equation 6 (in main text) giving $\{F_c = 0.13\pm0.02$ mN, $v_c = (3.4\pm1.5)\cdot10^3$ nm/s, $\Delta F = (36\pm7)\cdot10^{-3}$ mN$\}$. The blue curve is a fit with equation 7 (in main text) giving $n = 0.30\pm0.02$.

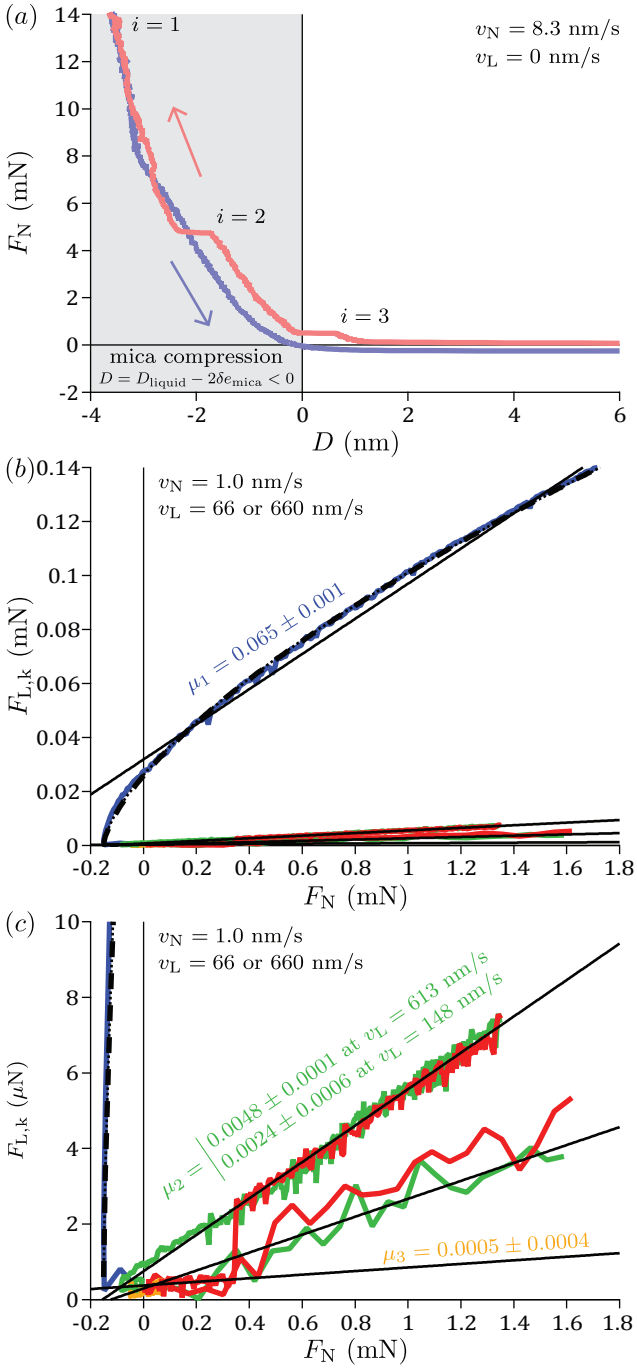

FIG. 7. Measurements for wet $[C_4C_1Pyrr][NTf_2]$, performed on different spots on the mica surfaces ($R = 1.14$ cm). (a) Normal force profile when approaching (in faded red) or retracting (in faded blue) the top surface with the stepper motor at $v_N = 8.3$ nm/s. (b) (c) Kinetic friction $F_{L,k}$ as a function of load F_N at different vertical scales, when moving the top surface with the piezoelectric tube at a normal velocity $v_N = 1.0$ nm/s and a lateral velocity $v_L = 660$ nm/s. The graphs show an approach up to layer $i = 2$ (in red), together with retractions from layers $i = 1$ (in blue), $i = 2$ (in green) and $i = 3$ (in orange). Straight lines are fits with the left-hand term of equation 4 (in main text), with $\{\mu_1 = 0.065 \pm 0.001$, $F_1^{min} = -0.49 \pm 0.02$ mN$\}$, $\{\mu_2 = 0.0048 \pm 0.0001$, $F_2^{min} = -0.16 \pm 0.01$ mN$\}$ and $\{\mu_3 = 0.0005 \pm 0.0004$, $F_3^{min} = -0.8 \pm 0.2$ mN$\}$. Friction clearly depends on lateral velocity in layer $i = 2$, with $\{\mu_2 = 0.0024 \pm 0.0006$, $F_2^{min} = -0.1 \pm 0.3$ mN$\}$ at $v_L = 148$ nm/s. The dotted line is a fit in layer $i = 1$ for the approach by discrete steps with the right-hand term of equation 4 (in main text), with $\{\sigma_{c,1} = 377.7 \pm 0.6$ kPa, $F_1^{min} = -0.15$ mN$\}$. The dashed line is a fit in layer $i = 1$ for the approach by discrete steps with the whole equation 4 (in main text), with $\{\mu_1 = 0.0013 \pm 0.0010$, $\sigma_{c,1} = 371 \pm 5$ kPa, $F_1^{min} = -0.15$ mN$\}$.

REFERENCES

[1] A. M. Smith, K. R. J. Lovelock, N. N. Gosvami, T. Welton, and S. Perkin, Phys. Chem. Chem. Phys. **15**, 15317 (2013).
[2] B. J. Briscoe, D. C. B. Evans, and D. Tabor, J. Colloid Interface Sci. **61**, 9 (1977).
[3] M. L. Gee, P. M. McGuiggan, J. N. Israelachvili, and A. M. Homola, J. Chem. Phys. **93**, 1895 (1990).
[4] H. Yoshizawa, P. McGuiggan, and J. Israelachvili, Science **259**, 1305 (1993).
[5] A. D. Berman, W. A. Ducker, and J. N. Israelachvili, Langmuir **12**, 4559 (1996).
[6] E. Kumacheva and J. Klein, J. Chem. Phys. **108**, 7010 (1998).
[7] C. Drummond and J. Israelachvili, Phys. Rev. E **63**, 041506 (2001).
[8] D. Gourdon and J. N. Israelachvili, Phys. Rev. E **68**, 021602 (2003).
[9] J. Gao, W. D. Luedtke, and U. Landman, J. Phys. Chem. B **102**, 5033 (1998).
[10] A. Socoliuc, E. Gnecco, S. Maier, O. Pfeiffer, A. Baratoff, R. Bennewitz, and E. Meyer, Science **313**, 207 (2006).
[11] P. A. Johnson, H. Savage, M. Knuth, J. Gomberg, and C. Marone, Nature **451**, 57 (2008).
[12] R. Capozza, A. Vanossi, A. Vezzani, and S. Zapperi, Phys. Rev. Lett. **103**, 085502 (2009).
[13] F. Giacco, E. Lippiello, and M. P. Ciamarra, Phys. Rev. E **86**, 016110 (2012).
[14] H. Lastakowski, J.-C. Géminard, and V. Vidal, Sci. Rep. **5**, 13455 (2015).
[15] H. Yoshizawa and J. Israelachvili, Thin Solid Films **246**, 71 (1994).
[16] R. M. Espinosa-Marzal, A. Arcifa, A. Rossi, and N. D. Spencer, J. Phys. Chem. Lett. **5**, 179 (2014).
[17] P. M. McGuiggan and J. N. Israelachvili, J. Mater. Res. **5**, 2232 (1990).
[18] M. Hirano, K. Shinjo, R. Kaneko, and Y. Murata, Phys. Rev. Lett. **67**, 2642 (1991).
[19] M. Ruths and S. Granick, Langmuir **16**, 8368 (2000).
[20] E. Charrault, X. Banquy, K. Kristiansen, J. Israelachvili, and S. Giasson, Tribol. Lett. **50**, 421 (2013).
[21] A. M. Smith, M. A. Parkes, and S. Perkin, J. Phys. Chem. Lett. **5**, 4032 (2014).
[22] R. M. Espinosa-Marzal, A. Arcifa, A. Rossi, and N. D. Spencer, J. Phys. Chem. C **118**, 6491 (2014).
[23] O. Y. Fajardo, F. Bresme, A. A. Kornyshev, and M. Urbakh, ACS Nano **11**, 6825 (2017).